

Supplementary Material:

The following is a flow chart to determine the partial $1/2\langle 101 \rangle$ dislocations on the (010) plane;

i.e. $\mathbf{b} = 1/2[101]$ and $\mathbf{b} = 1/2[-101]$.

1. The dislocation lines parallel to $[101]$ and $[-101]$ directions are long enough on the TEM foil (~ 200 nm thickness) along the $[010]$ zone axis, which are observed in WBDF images with $\mathbf{g} = 404$ and -404 (Figs. 2d, 2e and S1).
2. Determine 2 thickness contour fringes at the extremity of the dislocation with $\mathbf{g} = 400$ and 004 in the WBDF images (e.g., Fig. 3a).
3. $[001]$ dislocations can be dissociated to two pair of screw character $1/2\langle 101 \rangle$ dislocations on the (010) plane; $\mathbf{b} = 1/2[101]$ and $\mathbf{b} = 1/2[-101]$ (Fig. 4a).
4. The partial dislocations with Shockley-type stacking fault on the (010) plane are a glide configuration, which can contribute bulk strain in the simple-shear deformation and result in the development of the (010)[001] fabric in wadsleyite.
5. In addition, the $1/2\langle 101 \rangle$ dislocations are terminated on the edge of the (010) stacking faults. The partial dislocations was gliding in the (010) plane (Figs. 4b, S2 and S3).

Theoretical discussions on the glide of $1/2\langle 101 \rangle$ dislocations on the (010) planes

The glide mechanisms of $1/2\langle 101 \rangle$ partial dislocations can be theoretically supported as follows:

1. *Frank Criterion* (e.g., Sharp et al. 1994), 2. *Property of the (010) plane in the wadsleyite structure*, 3. *Short Burgers vector* (Table 1), and *Chalmers-Martius criterion* (Table 2). Length of Burgers vector and *d*-spacing are calculated using cell parameters of $(\text{Mg}_{0.9}, \text{Fe}_{0.1})_2\text{SiO}_4$ wadsleyite at ambient pressure-temperature conditions (Sawamoto and Horiuchi, 1990).

1. Frank Criterion

$$[001] \rightarrow \frac{1}{2}[101] + \frac{1}{2}[\bar{1}01]$$

$$|b_{\text{Perfect}}|^2 > |b_{\text{Partial (1)}}|^2 + |b_{\text{Partial (2)}}|^2$$

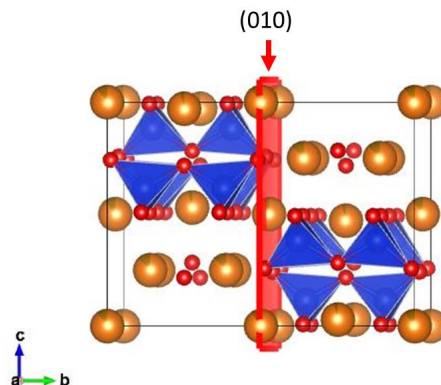
$$68.5 \text{ \AA}^2 \quad 50.6 \text{ \AA}^2$$

$$\text{(cf. } |b_{\text{Perfect}}|^2 = 32.6 \text{ \AA}^2 \text{ for } [100] \text{ dislocations)}$$

where the lattice parameters is $a = 5.7107(5) \text{ \AA}$, $b = 11.4675(9) \text{ \AA}$, $c = 8.2778(10) \text{ \AA}$.

2. Property of the (010) plane in the wadsleyite structure

The stacking fault plane is not an Oxygen sub-lattice, but a defective stacking sequence of the Magnesium cations (orange largest balls), which indicates a red plane in the figure below. The crystal structure was drawn with software VESTA (Momma and Izumi 2011).



No shearing SiO_4 (blue) and large *d*-spacing of the (010) plane

3. Short Burgers vector and *Chalmers-Martius* criterion (Cordier 2002)

TABLE 1. Length of Burgers vectors

| b | b (Å) |
|----------|--------|
| 1/2<101> | 5.03 |
| [100] | 5.71 |
| 1/2<111> | 7.63 |
| [001] | 8.28 |
| <101> | 10.06 |
| [010] | 11.47 |

TABLE 2. |b| / d_{hkl} ratio

| Slip System | b / d _{hkl} |
|----------------|-----------------------|
| 1/2<101> (010) | 0.44 |
| [100] (010) | 0.50 |
| [100] (001) | 0.69 |
| [100] {011} | 0.85 |
| <101> (010) | 0.88 |
| [100] {021} | 1.21 |
| [010] (001) | 1.39 |
| 1/2<111> {101} | 1.62 |
| [010] {101} | 2.44 |

REFERENCES CITED

- Cordier, P. (2002) Dislocations and slip systems of mantle minerals. In S. Karato, and H.-R. Wenk, Eds. *Plastic Deformation of Minerals and Rocks*, 51, 137-179. American Mineralogical Society, Washington DC.
- Momma, K., and Izumi, F. (2011) VESTA 3 for three-dimensional visualization of crystal, volumetric and morphology data. *Journal of Applied Crystallography*, 44, 1272-1276.
- Sawamoto, H., and Horiuchi, H. (1990) Beta (Mg_{0.9}, Fe_{0.1})₂SiO₄ - Single-Crystal Structure, Cation Distribution, and Properties of Coordination Polyhedra. *Physics and Chemistry of Minerals*, 17(4), 293-300.

Sharp, T.G., Bussod, G.Y.A., and Katsura, T. (1994) Microstructures in Beta-Mg_{1.8}Fe_{0.2}SiO₄ Experimentally Deformed at Transition-Zone Conditions. *Physics of the Earth and Planetary Interiors*, 86(1-3), 69-83.

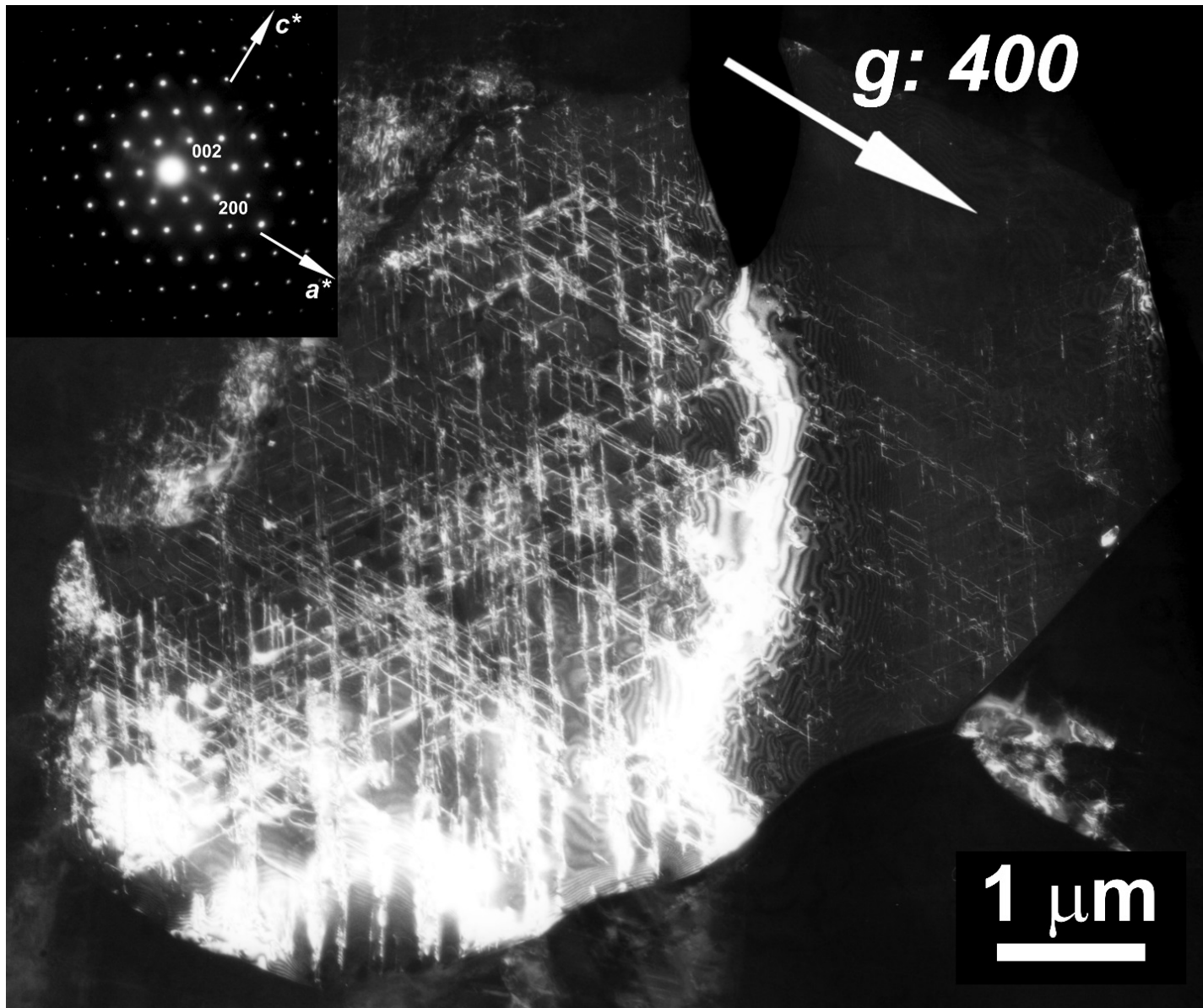
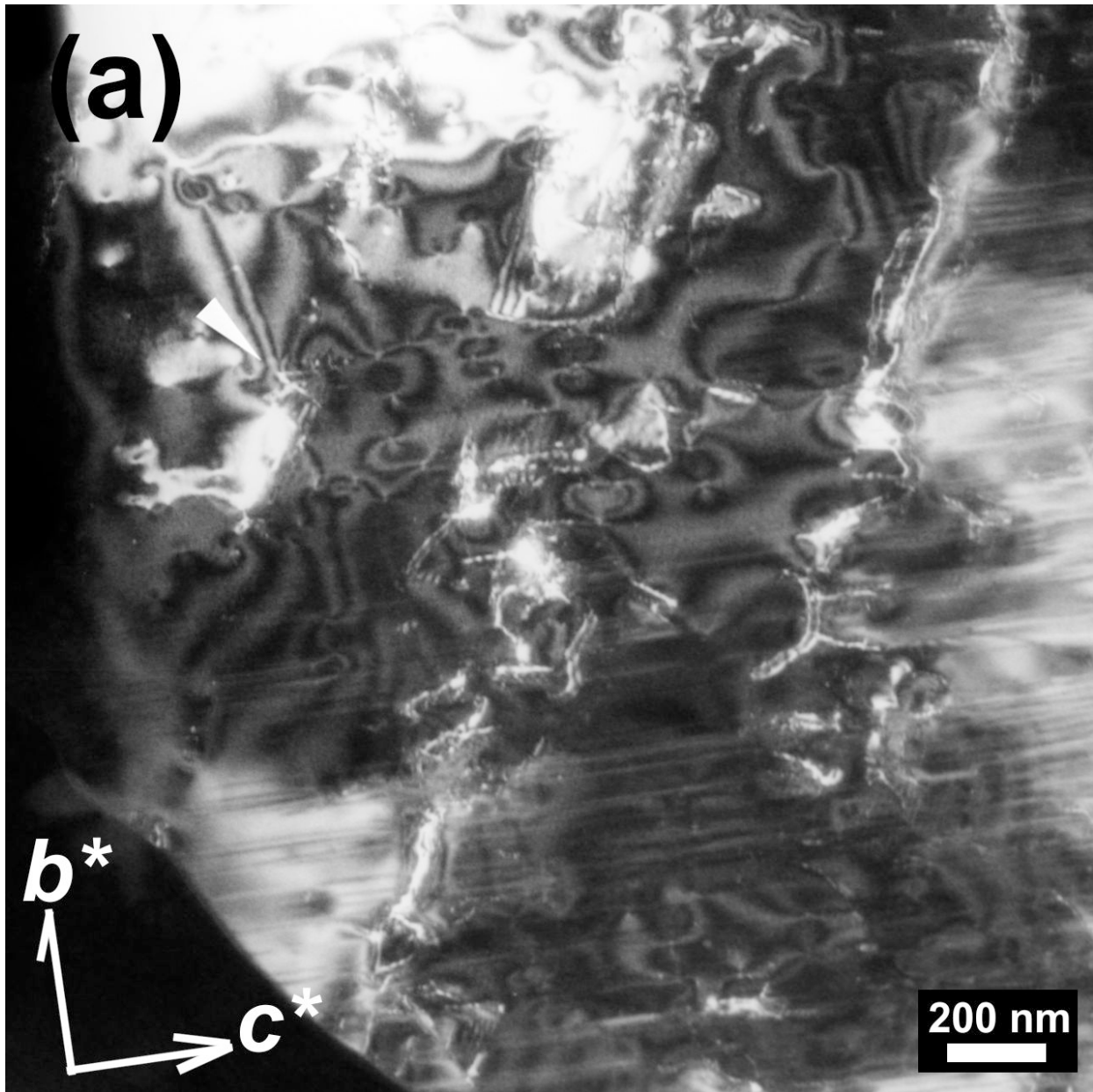


Figure S1. The WBDF image with $g = 400$ is taken from the same grain as that of the Figure 2.



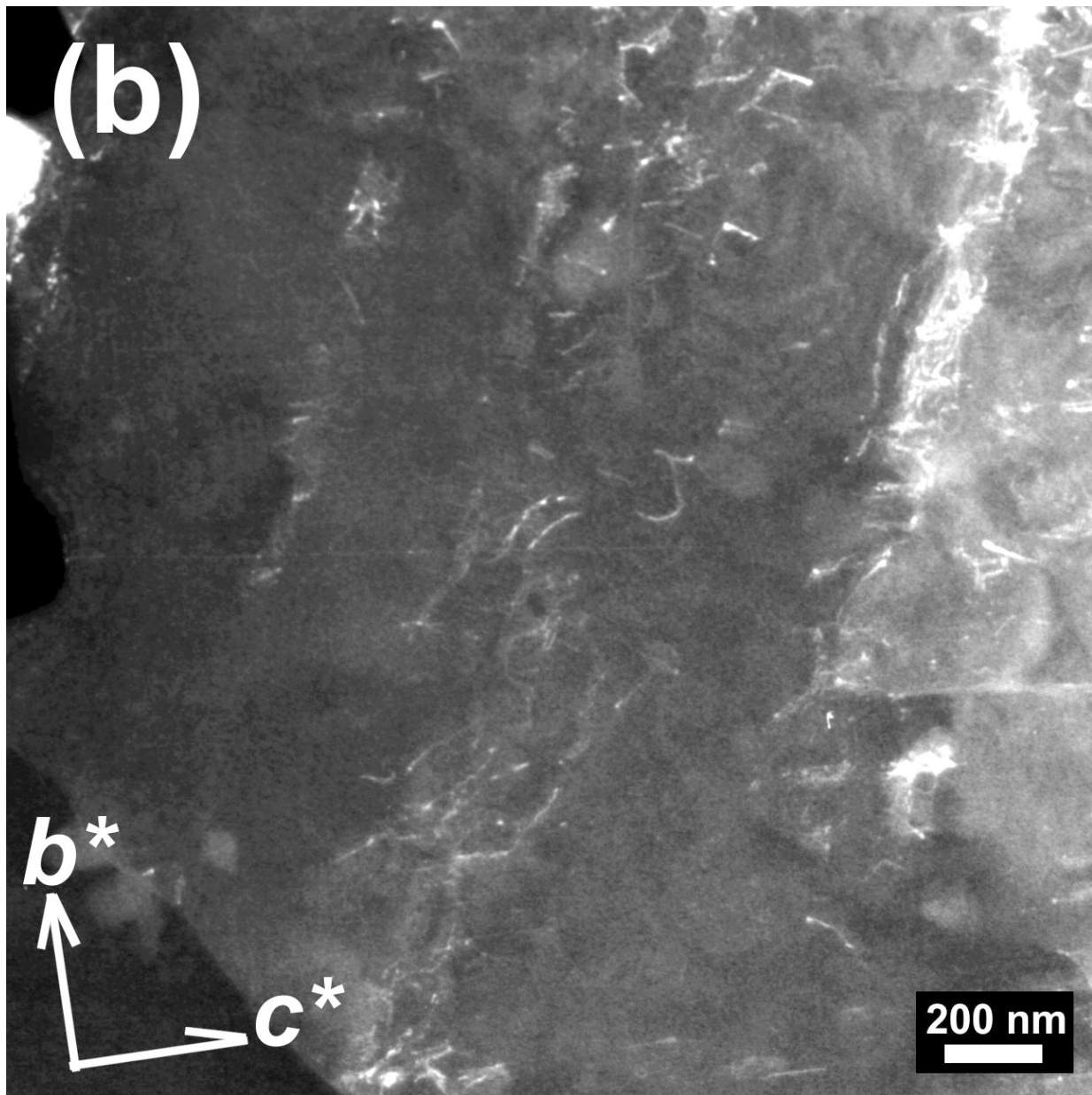
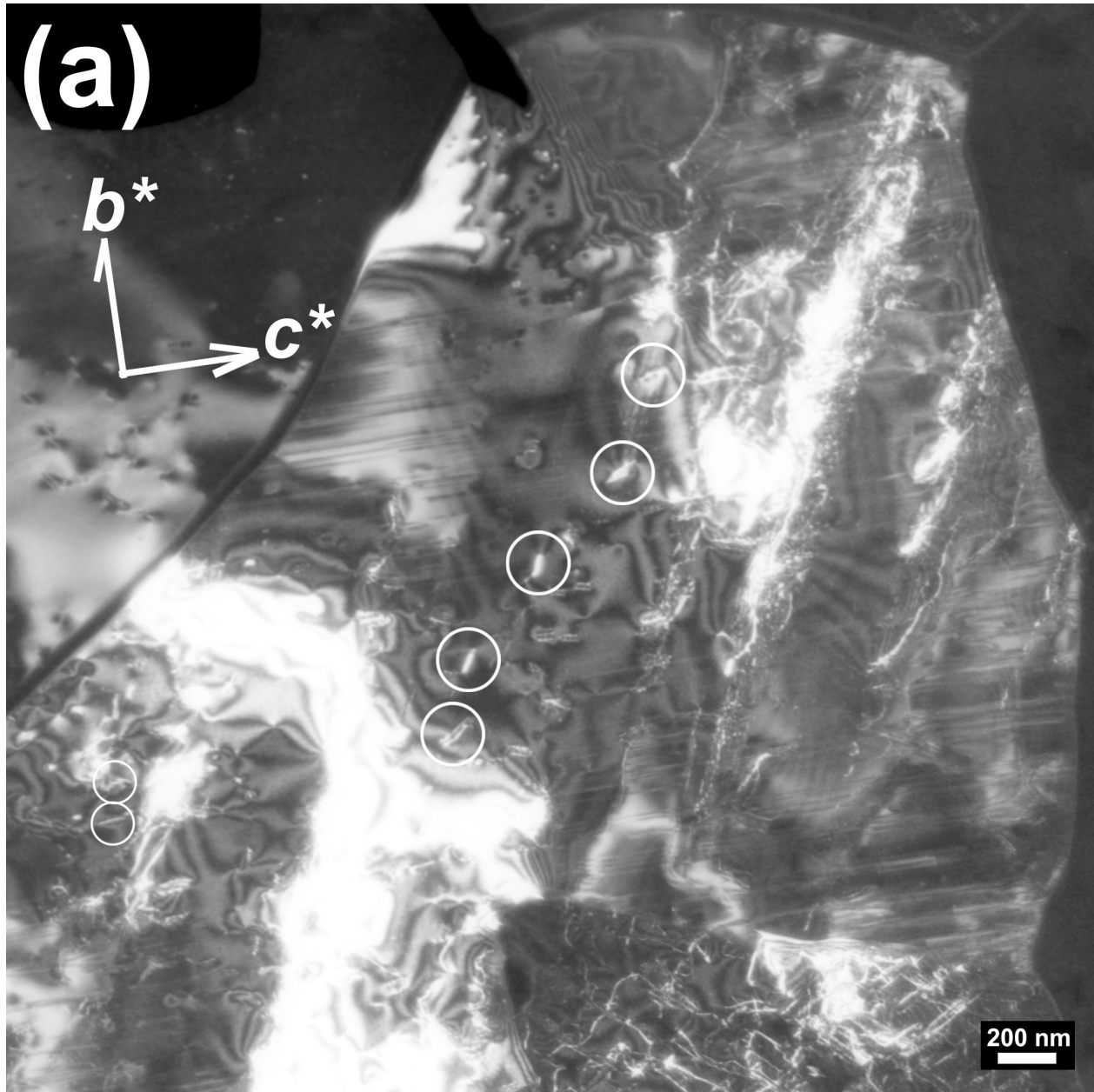
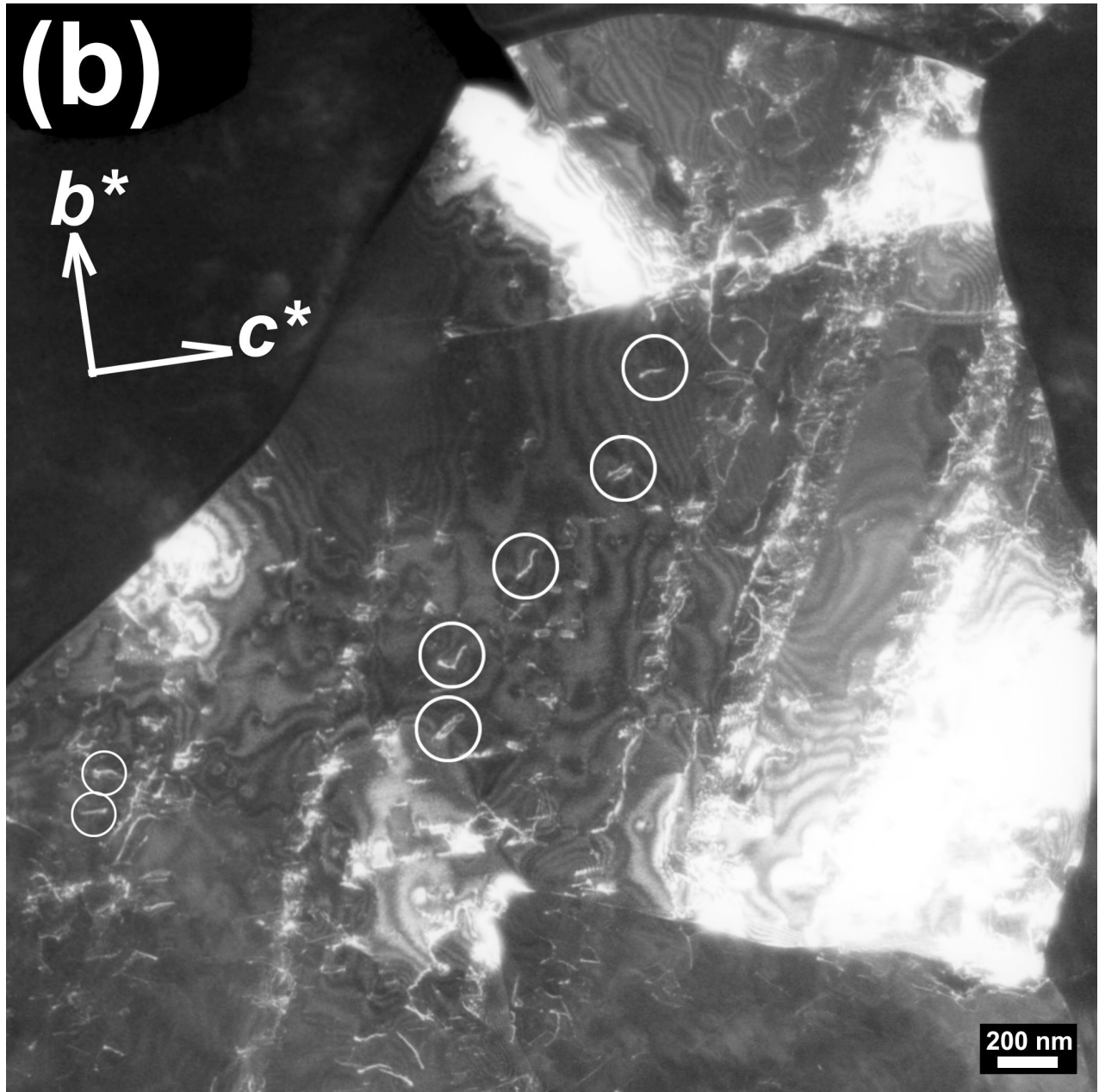


Figure S2. The WBDF image with (a) $g = 004$ and (b) $g = 080$ are taken from the same grain as that of the Figure 4b. The white arrow indicates the same dislocation in the Figure 4b.





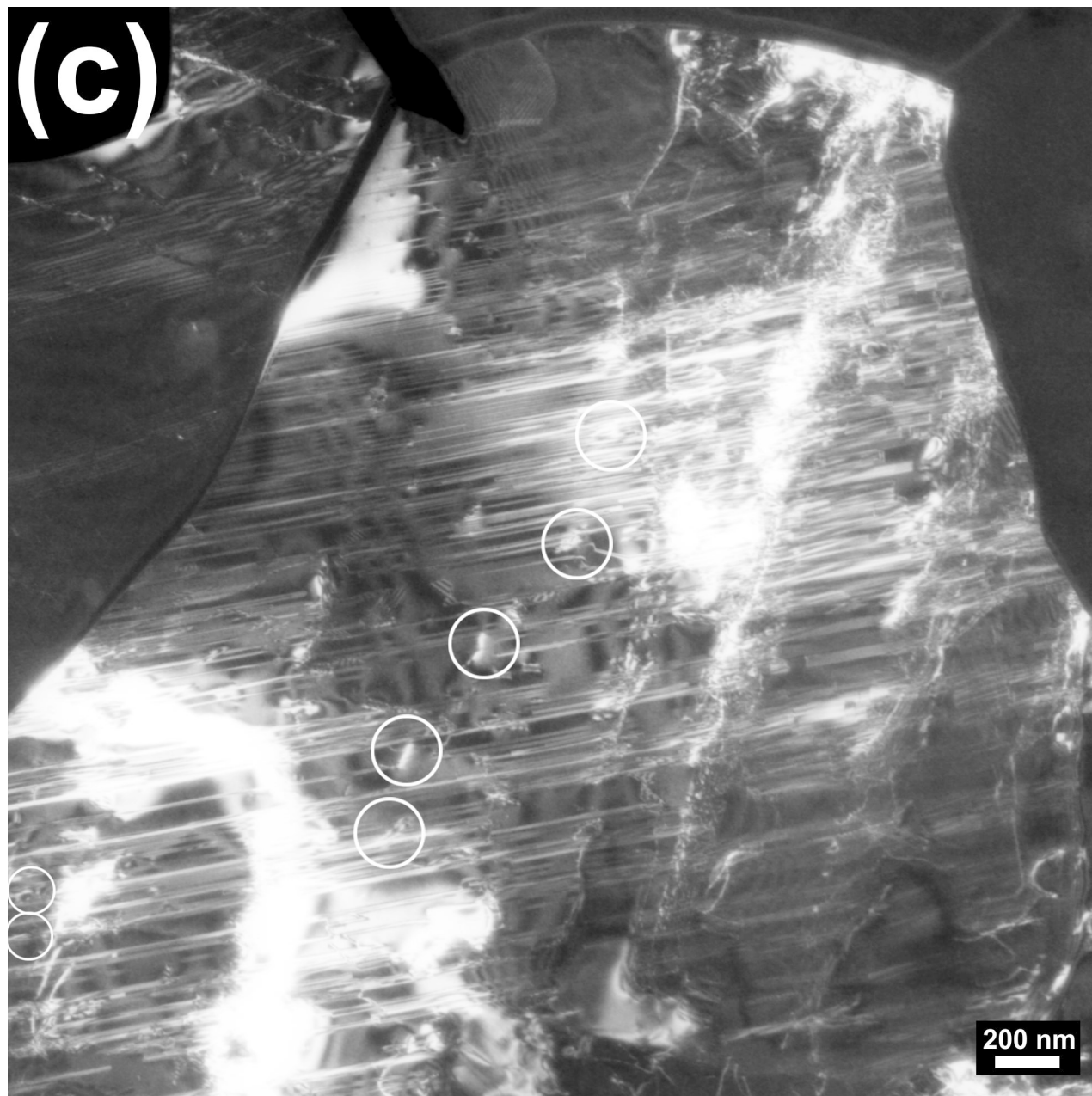
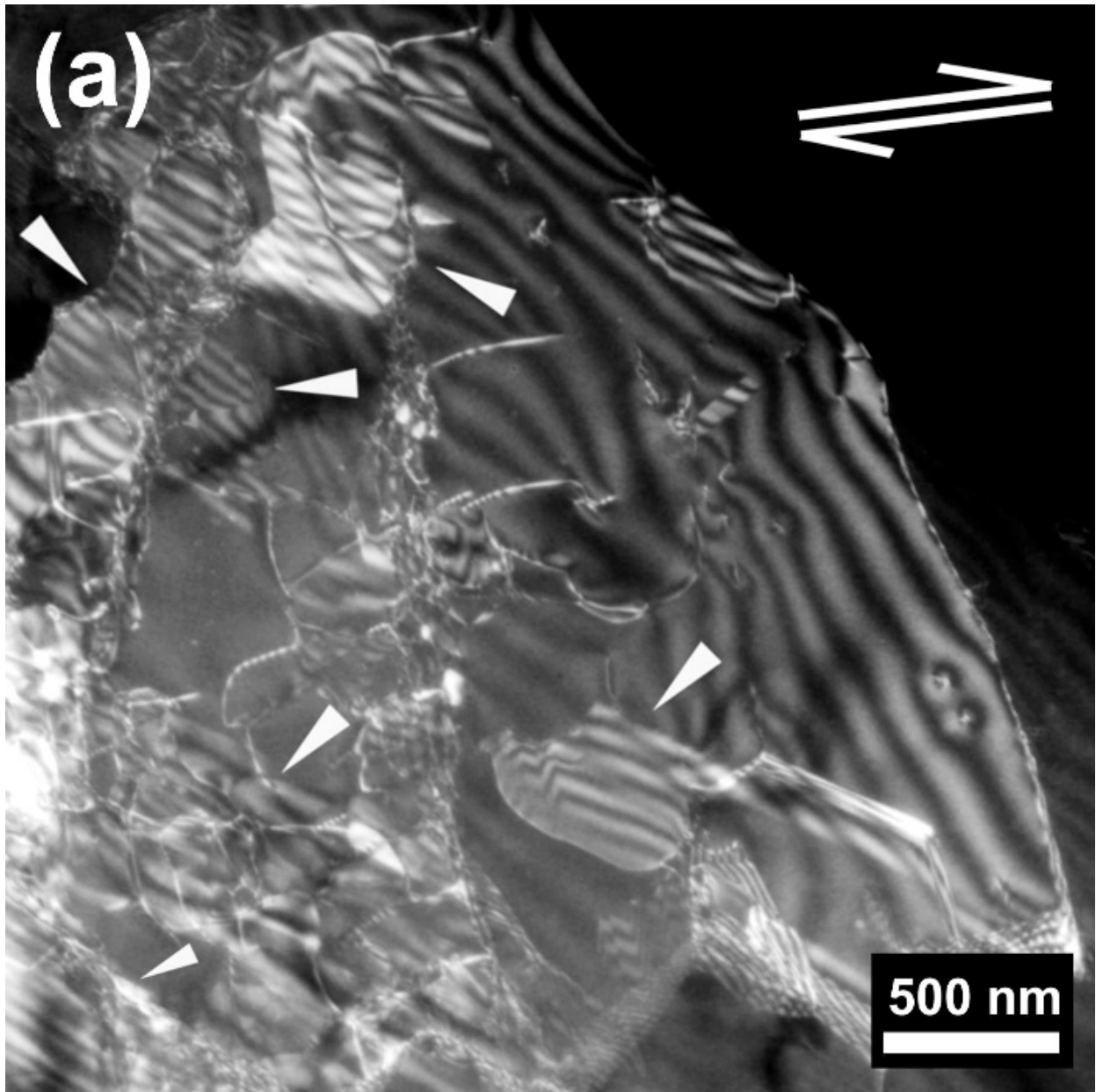


Figure S3. The WBDF image with (a) $g = 004$, (b) $g = 080$ and (c) $g = 013$ are taken from the same grain as that of the Figure 4b. The white cycles indicate the same dislocations in all three images, which are potentially included in a type of dislocations with $b = 1/2\langle 111 \rangle$.



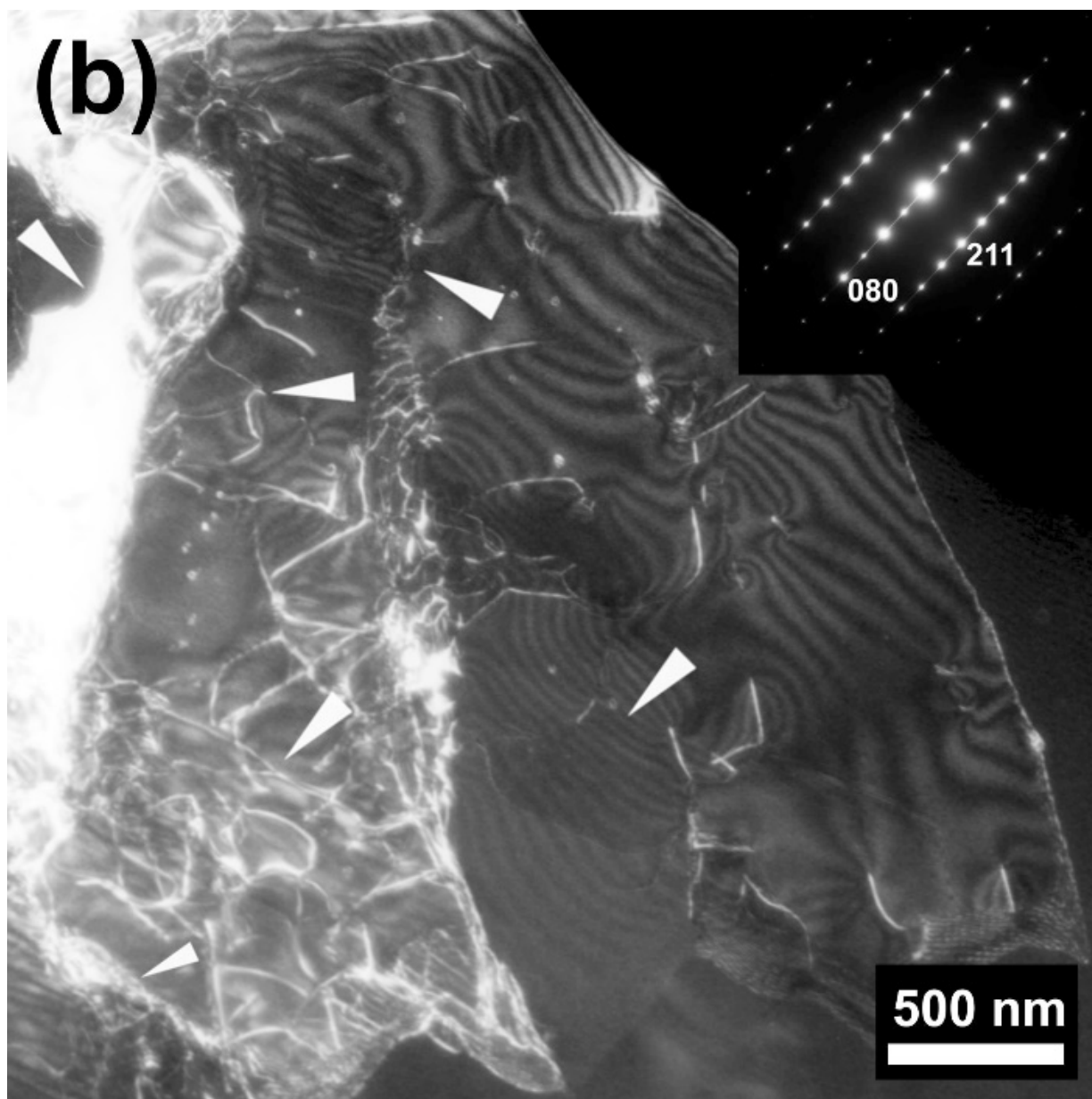


Figure S4. Typical dark field TEM images of non-deformed wadsleyite (run M0187 in Kawazoe et al. 2013). (a) $\mathbf{g} = \bar{2} \bar{1} \bar{1}$, stacking faults are visible, (b) $\mathbf{g} = 0\bar{8}0$, invisible. Some planar areas in the grain display fringe contrast of stacking faults (indicating white arrowheads) with partial dislocations at the ends, but they are not a glide configuration in contrast to Figure 4b where the (010) stacking fault planes are sub-parallel to a shear direction. The inset in the (b) is the nearest zone axis. The two-sided arrow on the upper right in (a) indicates a potential bulk shear direction.

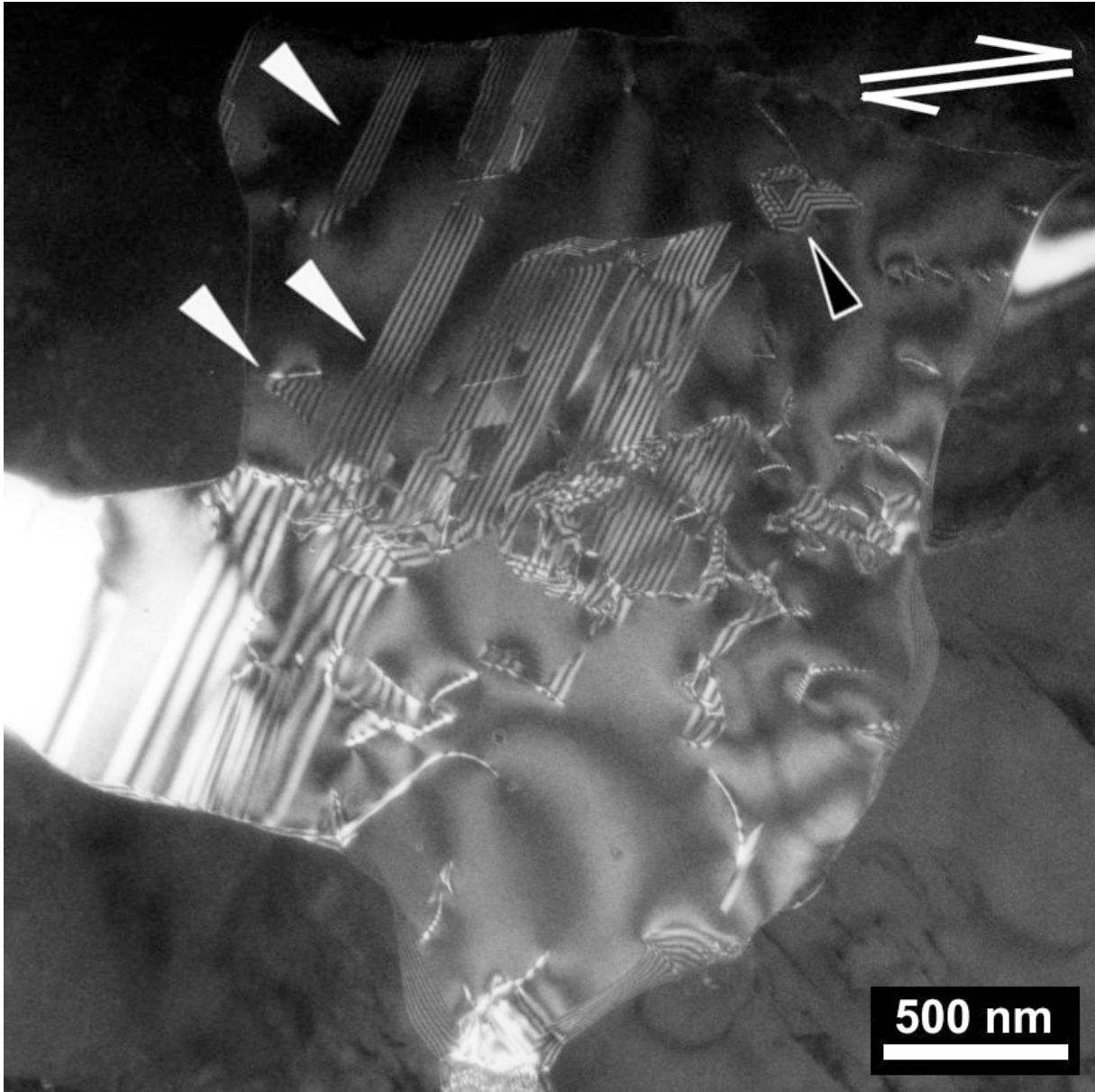


Figure S5. Dark field TEM image of non-deformed wadsleyite (M187), indicating a number of ledges (indicating black arrowheads) on the stacking faults (white arrowheads). The both side arrow on the upper right indicates a potential bulk shear direction.